THE JOURNAL OF PHYSICAL CHEMISTRY A

Article

pubs.acs.org/JPCA

Mechanism of Photo-Oxidation of Heptafluorobutyric Anhydride in the Presence of NO_2. Synthesis and Characterization of Heptafluoropropyl Peroxynitrate, $CF_3CF_2CF_2OONO_2$

Adriana G. Bossolasco, Fabio E. Malanca,* Maxi A. Burgos Paci, and Gustavo A. Argüello

Instituto de Investigaciones en Físico Química de Córdoba (INFIQC) CONICET-UNC, Departamento de Físico Química, Facultad de Ciencias Químicas, Universidad Nacional de Córdoba, Ciudad Universitaria, X5000HUA Córdoba, Argentina

Supporting Information

ABSTRACT: The photolysis of heptafluorobutyric anhydride at 254 nm in the presence of NO_2 and O_2 has been studied. It leads to the formation of $CF_3CF_2CF_2OONO_2$, $CF_3CF_2OONO_2$, and CF_2O as the only fluorine-containing carbonaceous products. The formation of the new heptafluoropropyl peroxynitrate (HFPN, $CF_3CF_2CF_2OONO_2$), as one of the main products, is a consequence of the formation of $CF_3CF_2CF_2OO^•$ radicals followed by the reaction with NO_2. To characterize HFPN, the UV absorption cross sections and their temperature dependence between 245 and 300 K have been measured over the wavelength range 200−300 nm as well as the infrared absorption cross sections. Kinetic parameters for its thermal decomposition are also presented in the temperature range between 281 and 300 K. The Rice−Ramsperger−Kassel−Marcus calculation reveals that the rate coefficient for the thermal decomposition at 285 K is almost independent of total pressure. The mechanism for the decomposition of $CF_3CF_2CF_2OONO_2$ in the presence of NO was adjusted by a kinetic model, which enabled the calculation of important rate coefficients.

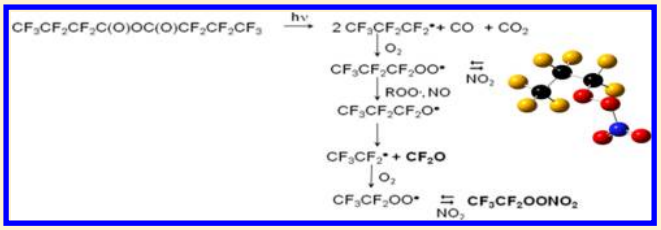

INTRODUCTION

Perfluoroperoxy radicals ($C_xF_{2x+1}OO^•$) are formed in the degradation of chlorofluorocarbons (CFCs), hydrofluorocarbons (HFCs), and hydrofluoroethers (HFEs), a series of compounds used as refrigerants, blowing and cleaning agents, emulsifiers, and solvents in general. In particular, perfluoropropyl peroxy radicals could be formed in the atmospheric oxidation of molecules containing $CF_3CF_2CF_2$ fragments such as HFC-227ca ($CF_3CF_2CF_2H$)[1] and *n*-perfluoropropyl formate (*n*-$CF_3CF_2CF_2$-OC(O)H).

As for other peroxy radicals ($ROO^•$), the atmospheric fate of $CF_3CF_2CF_2OO^•$ radicals is the reactions with NO, NO_2, HO_2, as well as other peroxy radicals ($ŔOO^•$).[1,2]

$$CF_3CF_2CF_2OO^• + NO \rightarrow CF_3CF_2CF_2O^• + NO_2 \quad (1a)$$

$$CF_3CF_2CF_2OO^• + NO + M \rightarrow CF_3CF_2CF_2ONO_2 + M \quad (1b)$$

$$CF_3CF_2CF_2OO^• + NO_2 + M \rightarrow CF_3CF_2CF_2OONO_2 + M \quad (2)$$

$$CF_3CF_2CF_2OO^• + HO_2^• \rightarrow \text{products} \quad (3)$$

$$CF_3CF_2CF_2OO^• + ROO^• \rightarrow \text{products} \quad (4)$$

Among the preceding reactions, reaction 2 leads to the formation of $CF_3CF_2CF_2OONO_2$ that should, in turn, decompose via reaction −2, as any known peroxynitrate

$$CF_3CF_2CF_2OONO_2 \rightarrow CF_3CF_2CF_2OO^• + NO_2 \quad (-2)$$

Thus, heptafluoropropyl peroxynitrate (HFPN, $CF_3CF_2CF_2$-$OONO_2$) could act as a reservoir species in the atmosphere, sequestering $ROO^•$ radicals and NO_2 and converting them into less reactive, electron paired, thermally stable molecules which at the same time could be transported from the source production site to remote places.

Reaction 2 has been studied by Giessing et.al,[1] who measured the rate coefficient for the reaction between $CF_3CF_2CF_2OO^•$ and NO_2 through pulse radiolysis and determined a value of $k_2 = (7.6 \pm 2.4) \times 10^{-12}$ cm^3 molecule^{-1} s^{-1}; however, no effort was made to evaluate the products of the reaction. In this work we went further and characterized the heptafluoropropyl peroxynitrate (HFPN, $CF_3CF_2CF_2OONO_2$) from infrared and UV spectra. Besides, we measured the temperature dependence of the ultraviolet absorption cross sections and the thermal stability as a function of both pressure and temperature. The study of the formation mechanism from the photolysis of heptafluorobutyl anhydride (HFBA) in the presence of NO_2 and O_2 was also performed. HFBA was only used as a clean source to provide the $C_3F_7^•$ radicals.

EXPERIMENTAL SECTION

Photolysis of $(CF_3CF_2CF_2C(O))_2O$ in the Presence of NO_2/O_2: Isolation and Recognition of $CF_3CF_2CF_2OONO_2$.

Received: July 19, 2012
Revised: September 4, 2012
Published: September 8, 2012

   dx.doi.org/10.1021/jp307172g | J. Phys. Chem. A 2012, 116, 9904−9910

Photolysis (λ= 254 nm) of mixtures of $(C_3F_7C(O))_2O/NO_2/O_2$ (0.7−1.0 mbar/0.3−0.5 mbar/610 mbar) were performed at room temperature (294 K) in a standard quartz infrared cell (23.0 cm path length), located in the optical path of a FTIR spectrophotometer which allowed us to monitor the appearance of products and the disappearance of reactants as a function of time.

The procedure used to synthesize $CF_3CF_2CF_2OONO_2$ is similar to that used to obtain the trifluoromethyl peroxynitrate by Chiappero et al.[3] The synthesis was conducted using a 10-L glass flask and keeping the temperature at 283 K. Typical pressures of $(C_3F_7C(O))_2O$, NO_2, and O_2 used were: 4.0, 2.5, and 1000 mbar, respectively. The progress was monitored every 30 min through infrared spectroscopy (transferring approximately 1% of the mixture to the IR cell each time), and photolysis was stopped when NO_2 concentration had decreased to a quarter of its initial value (approximately 2 h of irradiation). Scheme 1 shows the photochemical route after HFBA photolysis. The final resultant mixture was collected by slowly passing it through three traps kept at 87 K in order to remove excess O_2 and CO formed. It was

Scheme 1. Reaction Mechanism for HFBA Photolysis in the Presence of NO_2/O_2[a]

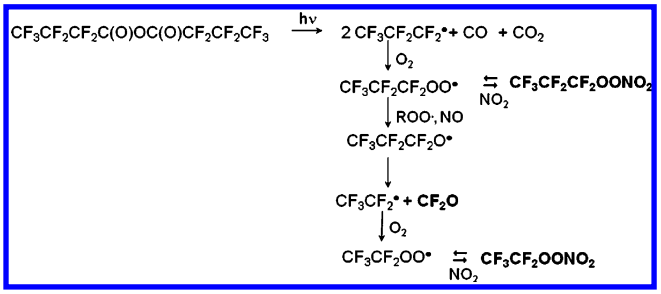

[a]Products observed and quantified are highlighted in bold.

then distilled between 188 and 153 K to eliminate the CF_2O and CO_2 formed. Further distillation between 213 and 173 K allows the separation of the HFBA that remains in the less volatile fraction. The more volatile fraction contains pure peroxynitrate. From this sample, reference IR spectra were taken.

To avoid HFPN decomposition, syntheses were carried out in the presence of sufficient NO_2 concentration to favor shifting the equilibrium

$$CF_3CF_2CF_2OONO_2 \leftrightarrows CF_3CF_2CF_2OO^{\bullet} + NO_2 \qquad (-2, 2)$$

toward the reactant and keeping the temperature at about 10 °C since its stability increases.

UV and IR Spectroscopy of $CF_3CF_2CF_2OONO_2$. Ultraviolet absorption spectrum of HFPN has been measured over the wavelength range 200−340 nm from 245 to 300 K using the experimental design described elsewhere.[4] Infrared spectra were recorded at room temperature with a resolution of 2 cm^{-1} averaging 16 scans in the range of 4000−400 cm^{-1}. The pressures ranged from 2.0 to 6.0 mbar for the UV and from 0.7 to 1.5 mbar for the IR spectra, respectively.

Absorption cross sections (σ) were determined according to

$$\sigma\ (cm^2\ molecule^{-1}) = 31.79 \times 10^{-20} (mbar\ cm^3\ molecule^{-1}\ K^{-1}) TA(pd)^{-1} \qquad (5)$$

where T is the temperature (K), A the absorbance, p the pressure (mbar), and d the optical path (cm).

Thermal Decomposition of $CF_3CF_2CF_2OONO_2$. Thermal stability was determined by monitoring, through FTIR, the temporal variation of the band at 997 cm^{-1} as a function of temperature and total pressure. Typical runs were carried out using 0.6−1.5 mbar of HFPN, 2.0 mbar of NO (that assures the capture of every peroxy radical formed), and N_2 up to the total pressure. Temperature dependence was studied between 281.0 and 300 K at 10 mbar of total pressure, while the pressure dependence study was performed at 284.2 K in the range from 10.0 to 600 mbar. Data at each temperature and pressure were analyzed according to a first-order rate law, maintaining a low conversion percentage. For each temperature, the decay was fitted by a linear regression and the value associated with the rate coefficient was plotted in the Arrhenius form.

Computational Details. Density functional theory has been used to evaluate the ground-state geometric parameters, vibrational frequencies, and the relative conformers populations of HFPN. The geometries, harmonic vibrational frequencies, and zero-point energies of the conformers were calculated using the hybrid density functional B3LYP with the 6-311+G* basis set. Density functional theory (DFT) methods take into account electron correlation energy to a partial extent,[5] and the particular method selected (though with a smaller basis set) has been extensively applied to the determination of geometric parameters of related oxygenated fluorocarbon compounds, yielding results that have been contrasted with gas electron diffraction experiments.[6−8] B3LYP/6-311+G* was used also for the determination of the geometric and vibrorotational parameters of the transition state for the thermal decomposition of HFPN, needed in the evaluation of the rate coefficients within Rice−Ramsperger−Kassel−Marcus (RRKM) formalism. These calculations were run using the G09 program package[9] in conjunction with GaussView 5.0.[10]

Thermal rate coefficients and their pressure dependence for the unimolecular decomposition of HFPN were evaluated using standard RRKM theory implemented in the UNIMOL program.[11]

The KINTECUS program package[12] was used to run kinetics simulations. This program allows the fitting of the time variations in the concentration of reagents and products while optimizing selected rate coefficients according to the mechanism proposed.

RESULTS AND DISCUSSION

Photolysis of HFBA in the Presence of NO_2 and O_2. Figure 1 shows a set of infrared spectra from the photolysis of mixtures of $(C_3F_7C(O))_2O$, NO_2 and O_2 together with selected reference spectra. The first trace corresponds to the starting mixture. Appropriate subtraction of reactants to the trace obtained at 24 min of photolysis leads to the spectrum of the products (trace "A"), which shows the appearance of peaks corresponding to carbonyl fluoride and others (around 1760 and 790 cm^{-1}) compatible with fluorinated peroxynitrates ($ROONO_2$). The subtraction of carbonyl fluoride leads to a trace, which is the sum of the contribution of various peroxynitrates, mainly heptafluoropropyl peroxynitrate (HFPN, $CF_3CF_2CF_2OONO_2$) as can be seen by comparison of trace "C" with the spectrum of the pure compound "D". Further subtraction reveals the presence of another perfluorinated peroxynitrate, $CF_3CF_2OONO_2$, whose reference spectrum[13] is shown in trace "F".

These products could be explained taking into account that the rupture of the precursor molecule leads to the formation of CO, CO_2, and perfluorinated radicals ($CF_3CF_2CF_2^{\bullet}$) in a similar way to trifluoroacetic (TFAA)[14] and pentafluoro propionic anhydride

dx.doi.org/10.1021/jp307172g | J. Phys. Chem. A 2012, 116, 9904−9910

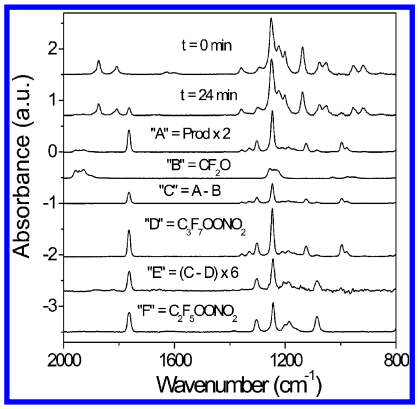

Figure 1. Photooxidation of PFBA in the presence of NO_2.

(PFPA).[15] As it is shown in Scheme 1, in general terms, perfluorinated radicals react with oxygen leading to the formation of peroxy radicals ($CF_3CF_2CF_2OO^\bullet$ or $CF_3CF_2OO^\bullet$), which in turn react with NO_2 leading to the formation of the corresponding peroxynitrates ($CF_3CF_2CF_2OONO_2$ or $CF_3CF_2OONO_2$, respectively). HFPN decomposes thermally to reform $CF_3CF_2CF_2OO^\bullet$ radicals, which could recombine or react with NO (formed by the photolysis of NO_2) to form alkoxy radicals that ultimately lead to formation of CF_2O.

Temporal variation of reactants and products are shown in Figure 2a. As expected, the concentration of CF_2O and peroxynitrates increases as time elapses. According to the mechanism proposed (Scheme 1) and the carbon balance derived from it, the rupture of the HFBA molecule leads to the following relationship

$$2\Delta p_{(CF_3CF_2CF_2C(O))_2O} = p_{CF_3CF_2CF_2OONO_2} + (p_{CF_2O} = p_{CF_3CF_2OONO_2}) \quad (6)$$

where p corresponds to the partial pressure (mbar) of each reactant or product.

Figure 2b shows the concentration of the products formed as a function of HFBA disappearance. The relative percentage values for the formation of $CF_3CF_2CF_2OONO_2$, CF_2O, and $CF_3CF_2OONO_2$ give 130 ± 9, 68 ± 5, and 65 ± 5, respectively. Taking into account the preceding relationship, the percentage of products observed explain about 98% of the disappearance of HFBA, in agreement with the non-observation of other fluorinated products (e.g., CF_3OONO_2).

DFT Calculations. The conformational space of HFPN can be described taking into account the five main dihedral angles of the skeleton F—CF_2—CF_2—CF_2—O—O—N—O_2, which can be reduced to four because φ_0(F—CF_2—CF_2—CF_2) always adopts the anti configuration. These four dihedrals are: φ_1(F_3C—CF_2—CF_2—O), the relative position of the CF_3 group with respect to the C—O bond; φ_2(F_3C—CF_2—CF_2—O—O), the relative position of the C_2F_5 fragment with respect to the peroxy bond; φ_3(C_3F_7—O—O—N), the relative position of the carbonaceous chain with respect to the O—NO_2 bond and φ_4(C_3F_7O—O—NO—O), the relative position of the NO_2 group with respect to the peroxy bond. Enantiomers are not taken into account because there is no energy difference between them. Dihedrals φ_1 and φ_2 could adopt sin (0°), anti (180°), or gauche (~60 or ~120°) configurations. Experimental and theoretical studies of similar peroxynitrates have shown that the X—O—O—Y and O—O—N═O dihedrals (φ_3 and φ_4 in our case) adopt gauche and syn configurations, respectively.[16,17] Within this analysis the minima of the configurational space can be reduced to the different possibilities of φ_1 and φ_2. A relaxed potential energy surface (PES) scan for the joint variation of φ_1 and φ_2 from 0 to 180° was run, and the result is shown as a contour map in Figure 3. The contour map was constructed by

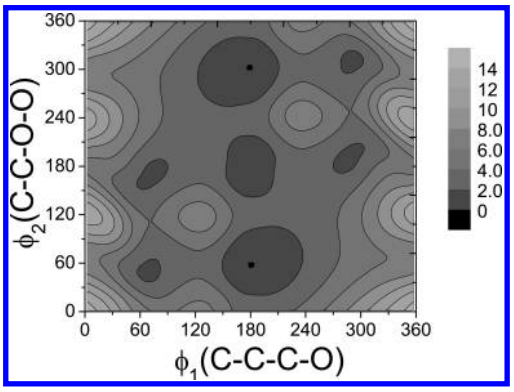

Figure 3. Relaxed PES scan for the joint variation of φ_1 and φ_2 from 0 to 360°.

appropriate reflections of the scanned points to show variations of 360° for each angle. Four different minima are found in the PES being the one with φ_1 = 180° and φ_2 = 56° the global minimum. These four minima are designated from **1** to **4** in ascending order of their relative energy. A qualitative inspection of the PES shows that interconversion between the minima could

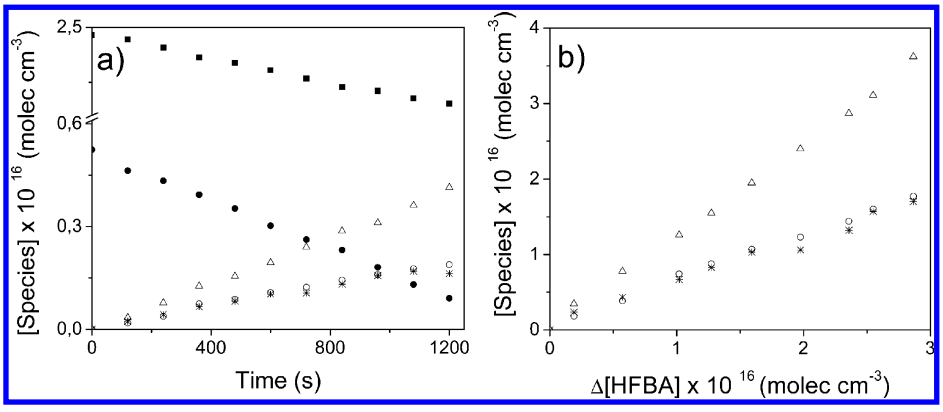

Figure 2. (a) Temporal variation of reactants and products in the photolysis of a mixture containing HFBA, NO_2, and O_2. Symbols correspond to $(C_3F_7C(O))_2O$ (■), NO_2 (●), $CF_3CF_2CF_2OONO_2$ (Δ), CF_2O (○), and $C_2F_5OONO_2$ (□). (b) Formation of products $CF_3CF_2CF_2OONO_2$ (Δ), CF_2O (○), and $C_2F_5OONO_2$ (□) as a function of PFBA disappearance.

dx.doi.org/10.1021/jp307172g | J. Phys. Chem. A 2012, 116, 9904−9910

involve trajectories needing less than 4 kcal mol^{-1} and that the relative energies are less than 1.8 kcal mol^{-1} with respect to **1** (Figure I in the Supporting Information depicts the structure of **1**). Table 1 in the Supporting Information shows the B3LYP/6-311+G* absolute energies together with the relative energies and room temperature populations for the rotamers. Relative populations were calculated according to the formula

$$N_x/N_1 = Q_1/Q_x \exp(-\Delta E/kT) \quad (7)$$

where Q_x is the total partition function, taken from G09, of rotamer x. It is noteworthy that the calculation anticipates a blend of the four rotamers at room temperature.

Table 1. Calculated Geometric Parameters of the Most Stable Conformer

geometric parameters			
$C_3F_7OONO_2$		CF_3OONO_2	GED
distance (Å)			
C—F (mean)	1.343	C—F	1.322
C—C (mean)	1.564		
C4—O5	1.386	C—O	1.378
O5—O6	1.411	O—O	1.414
O6—N7	1.560	O—N	1.523
N7═O(8.9)	1.182	N═O	1.187
angles (deg)			
F—C—F	108.9	F—C—F	108.8
C2—C3—C4	116.5		
C5—C8—O11	107.4		
C4—O5—O6	109.4	C—O—O	107.7
O5—O6—N7	108.9	O—O—N	108.4
O6—N7═O9	116.2		
O6—N7═O8	108.3		
O8═N7═O9	135.5	O═N═O	135.2
C2—C3—C4—O5	−56.7		
C3—C4—O5—O6	179.9		
C4—O5—O6—N7	104.7	φ(C—O—O—N)	105.1
O5—O6—N7—O8	178.1	φ(O—O—N═O3)	178.3
O5—O6—N7—O9	0.9		

Table 1 shows the geometrical parameters for this rotamer together with the experimental GED results of the similar peroxynitrate, CF_3OONO_2.[18] The agreement between the calculated parameters with those in similar compounds is remarkable for the level of theory used. The most interesting parameters in peroxynitrates are the X—O—O—N dihedral and the O—N distance. Previous studies on peroxy compounds show that the dihedral is around 120° or 90° for two sp^3 or sp^2 substitutes, respectively, and 105° for one sp^3/sp^2 substitute, as is the case for peroxynitrates.[16,18] The calculated value of this parameter is 104.7° for HFPN, and it agrees well with this tendency. The N—O distance is extremely long in peroxynitrates, and it has been observed that it depends a lot on the electronegativity of the group attached to the $-ONO_2$ fragment. Values of 1.507 and 1.523 Å are reported for $FONO_2$ and CF_3OONO_2, respectively,[18,19] suggesting that the CF_3O group is more electronegative than F. In HFPN a value of 1.560 Å is found, and it can be thought that the C_3F_7O group is still more electronegative than CF_3O. A DFT calculation for $CF_3CF_2OONO_2$ with the same basis set gives 1.560 Å for the O—N distance, showing that addition of more CF_3 groups to the carbon chain does not influence the O—N distance. Although the absolute DFT value of 1.560 Å is really long and it involves an uncertainty of ∼2%, it is very interesting that it anticipates an even longer N—O distance for HFPN than for CF_3OONO_2. An experimental GED study for this molecule is really desirable.

UV and IR Absorption Cross Sections. Figure 4 shows the experimental infrared absorption cross sections in the range of 2000 to 600 cm^{-1}, for CF_3OONO_2,[18] $CF_3CF_2OONO_2$,[13] and $CF_3CF_2CF_2OONO_2$ (first, second, and third traces) and the theoretical unscaled spectrum calculated for $CF_3CF_2CF_2OONO_2$ (bottom trace). As can be seen, the HFPN spectrum is in agreement with the general trend shown by many peroxynitrates. However, there is a distinguishable signature present in the HFPN at 996 cm^{-1} that allows its differentiation from the other fluorinated peroxynitrates, and that was used for its identification and quantification. The infrared bands (in units of cm^{-1}), the corresponding absorbance cross sections ($\sigma \times 10^{18}$, cm^2 $molecule^{-1}$), and their assignment for the main peaks are 1764 (3.1 ± 0.1) ν_{as} (NO_2), 1302 (1.58 ± 0.06) ν_s (NO_2), 1246 (5.7 ± 0.1) ν_{as} (CF_3), 1125 (1.28 ± 0.05) ν_{as} (C—F), 996 (1.43 ± 0.05) ν_s (O—O), and 790 (1.19 ± 0.05) def. δNO_2. As stated before, four different rotamers should be in equilibrium in a gas-phase sample of HFPN at room temperature, according to the DFT calculation. Because of this, the theoretical spectrum shown in the bottom of Figure 4 was synthesized from the linear combination of the theoretical spectrum of each rotamer multiplied by the corresponding population. Every vibrational transition was modeled with a Lorentzian function with 4 cm^{-1} of fwhh. The comparison between the experimental and theoretical spectra shows a good correlation for the featured peaks.

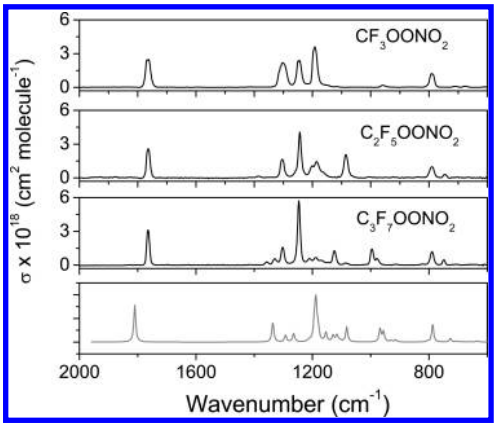

Figure 4. Infrared absorption cross sections for $C_xF_{2x+1}OONO_2$, $x = 1-3$. The bottom trace (gray line) corresponds to the simulated $CF_3CF_2CF_2OONO_2$ spectrum.

Figure 5 shows the UV spectrum of $CF_3CF_2CF_2OONO_2$ between 200 and 300 nm and its temperature dependence in the range from 245 to 300 K; meanwhile Table 2 of Supporting Information summarizes the absorption cross sections at different temperatures. As can be seen the UV absorption cross sections increase with the temperature. This increment is consistent with an increased population of the vibrational and rotational levels of the ground electronic state of the molecule at higher temperatures.[20]

The temperature dependence is more pronounced toward the longer wavelength tail as shown in the representation of $\log(\sigma)$ vs T, which leads to linear fits according to $\log(\sigma) = BT + \log(\sigma_0)$, where σ and σ_0 are the cross sections (cm^2 $molecule^{-1}$) at T and 0 K, respectively. The intercepts $\log(\sigma_0)$ and slopes (B) obtained

dx.doi.org/10.1021/jp307172g | J. Phys. Chem. A 2012, 116, 9904−9910

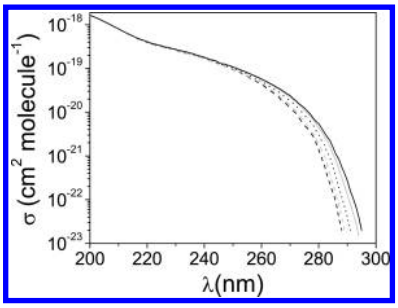

Figure 5. UV spectra of $CF_3CF_2CF_2OONO_2$ at different temperatures: 245 K, dashed black; 253 K, dashed gray; 268 K, dotted; 283 K, solid gray; 300 K, solid black.

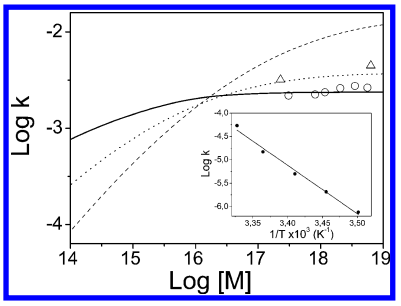

Figure 6. Dependence of the rate coefficient with pressure for $C_xF_{2x+1}OONO_2$ obtained from RRKM calculations (x = 1, dashed line; x = 2 dash−dotted line; x = 3, solid line) and from experimental data (x = 2, triangles; x = 3, circles).The insert shows the Arrhenius plot for the thermal decomposition of $CF_3CF_2CF_2OONO_2$ at 10.0 mbar of total pressure between 284 and 300 K.

by linear regression analysis for the wavelength range 200−285 nm are given in Table 3 of the Supporting Information As can be seen, B increases with wavelength as a consequence of the larger temperature dependence at longer wavelengths.

Thermal Stability of $CF_3CF_2CF_2OONO_2$: Kinetic Modeling. The thermal stability was studied between 281 and 300 K at 10.0 mbar of total pressure. The rate coefficient values for the peroxynitrate decomposition (reaction −2) were corrected considering that, as time elapses, the NO added leads to an increase in NO_2 formation, slightly shifting the equilibrium toward the formation of $CF_3CF_2CF_2OONO_2$ via reaction 2. The equation used to correct the rate coefficient has been reported elsewhere.[21]

$$k_{-2} = k_{obs}\left(1 + \frac{k_2[NO_2]}{k_1[NO]}\right) \quad (8)$$

where k_{obs} corresponds to the uncorrected experimental rate of disappearance of $CF_3CF_2CF_2OONO_2$. The ratio k_2/k_1 was determined using the values for the rate coefficients determined by Giessing et al.[1]

Master equation calculations within the RRKM formalism were run to evaluate the pressure dependence of the rate coefficient. The model used involves the following approximations. Intermolecular collisions of the peroxynitrate with the buffer gas (N_2 in all cases) take place under a Lennard-Jones potential. The critical parameters were estimated by the methods in chapter 6 of Gilbert and Smith.[22] The values obtained are σ_{LJ} = 6.45 Å and σ_{LJ} = 3.9 Å for HFPN and N_2, respectively. All internal modes and moment of inertia of the reagent and TS were taken from the DFT calculations. All internal modes were treated as active vibrations and multiplied by the scale factor 1.0013 as suggested by Scott and Radom.[23] The external rotation of lowest moment of inertia was treated as fully active and the two remaining as adiabatic modes. Rate coefficients are very sensitive to the critical energy, and there is a difference of more than 1 kcal mol^{-1} between the calculated and experimental values. Although this is acceptable for the evaluation of a bond fission reaction at the B3LYP/6-311+G* level, for modeling kinetics parameters more precision is needed, and because of this we decided to use the experimental value of the activation energy. A Morse potential was fitted to evaluate the ROO···NO_2 interaction using the experimental activation energy and the proper stretching frequency.

In turn, Figure 6 shows the experimental dependence of the rate coefficient with pressure (12 to 220 mbar at 284 K) and its comparison with the results obtained from RRKM for $C_xF_{2x+1}OONO_2$ (x = 1, 2, 3) using the UNIMOL program suite.[11] As can be seen, the rate coefficient for x = 3 (i.e., HFPN) shows a slight dependence with the pressure, and its value ranges between 2.1 and 2.5 × 10^{-3} s^{-1}. For x = 2, the pressure dependence is stronger and for x = 1 even stronger. A good agreement between the experimental and calculated data can be observed for pressures higher than 1 mbar, while for pressures lower than 1 mbar, the dependence with the length of the carbon chain is reversed.

Arrhenius parameters derived from a plot of ln k vs $(1/T)$ (inset of Figure 6), at 10.0 mbar total pressure, are: activation energy (E_a = 84.9 kJ/mol) and pre-exponential factor (A = 1.0 × 10^{13}). The comparison (E_a and A) for the series $C_xF_{2x+1}OONO_2$ (x = 1, 2, 3) (90.8 and 1.05 × 10^{14}),[24] (87.7 and 3.8 × 10^{13}),[13] (84.9 and 1.0 × 10^{13}) kJ/mol, respectively, shows that E_a decreases as the length of the perfluorinated alkyl group increases, thus, the longer the chain, the shorter the lifetime, consistent with the trends of the calculated and experimental values (see Figure 6) for pressures higher than 1 mbar.

Table 2 shows the mechanism proposed for the thermal decomposition, according to the products observed. The values for the rate coefficients were obtained either from the literature or adjusted with the KINTECUS model. The most relevant to note is that (a) the value for k_{IV} is in agreement with the value suggested by Giessing et. al (>1.5 × 10^5 s^{-1}) and (b) the values for k_{VI}, which resulted from the fit of the kinetic model to the experimental points and are reported for the first time in this work, are consistent with the reported values for similar reactions.[25] The good fit obtained is presented in Figure 7.

Atmospheric Implications. Photochemistry of HFBA in the presence of NO_2 and O_2 leads to the formation of a new peroxynitrate, HFPN, a compound whose stability is similar to other fluorinated alkyl peroxynitrates $C_xF_{2x+1}OONO_2$ (x = 1, 2) and that follows the expected trends.

The loss of peroxynitrates in the atmosphere occurs through different processes, namely thermal decomposition, photolysis, and reaction with OH radicals, whose relative importance depend on the region of the atmosphere and the very nature of the peroxynitrate.[26] In particular, HFPN is unstable at temperatures of the free troposphere, and its thermal lifetime should be of the order of minutes. At altitudes higher than 5 km, where the temperatures are lower than 250 K, its stability increases to achieve a thermal lifetime of one year at the tropopause; beyond 20 km it should start decreasing. However, between 10 and 30 km, the thermal lifetime should be higher than 3 months and considering the atmospheric horizontal mixing at these altitudes HFPN would be transported for long distances.

dx.doi.org/10.1021/jp307172g | J. Phys. Chem. A 2012, 116, 9904−9910

Table 2. Reaction Mechanism of HFPN Decomposition in the Presence of NO and Rate Coefficients Used in the Kinetic Model (KINTECUS)

	reaction	k	reference
I	$CF_3CF_2CF_2OONO_2 \rightarrow CF_3CF_2CF_2OO^{\bullet} + NO_2$	2.1×10^{-3}	this work
II	$CF_3CF_2CF_2OO^{\bullet} + NO_2 \rightarrow CF_3CF_2CF_2OONO_2$	7.6×10^{-12}	Wallington, 1996
III	$CF_3CF_2CF_2OO^{\bullet} + NO \rightarrow CF_3CF_2CF_2O^{\bullet} + NO_2$	9.0×10^{-12}	Wallington, 1996
IV	$CF_3CF_2CF_2O^{\bullet} \rightarrow CF_3CF_2^{\bullet} + CF_2O$	1.0×10^{6}	this work
V	$CF_3CF_2^{\bullet} + NO \rightarrow CF_3CF_2NO$	1.5×10^{-12}	this work
VI	$CF_3CF_2^{\bullet} + NO_2 \rightarrow CF_3C(O)F + FNO$	1.8×10^{-11}	this work
VII	$FNO + wall \rightarrow HF + NO_2$	1.0×10^{-1}	

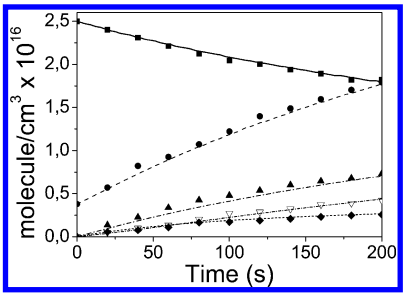

Figure 7. Temporal variation of reactants and products in the thermal decomposition of HFPN: (■) $CF_3CF_2CF_2OONO_2$, (▲) CF_2O, (▽) CF_3COF, (●) NO_2, and (♦) CF_3CF_2NO. Lines represent the best fit given by the KINTECUS model.

The UV absorption cross sections at wavelengths shorter than 300 nm are relevant for the photochemical lifetime estimation. Taking into account the altitude profile of UV wavelengths and that HFPN starts absorbing mainly at wavelengths shorter than 300 nm, its photochemical rupture begins to take importance from 35 km up, reaching values about minutes at altitudes higher than 40 km. Therefore the thermal decomposition prevails over the photochemical rupture from the surface until about 40 km.

Comparison with the lifetime of the most abundant peroxynitrate measured in the atmosphere, PAN $-CH_3C(O)-OONO_2-$ (from minutes in free troposphere to 20 days at tropopause)[27] reveals that this new peroxynitrate could be formed in the atmosphere and act as a reservoir of NO_2 and peroxy radicals.

■ ASSOCIATED CONTENT

Ⓢ Supporting Information

The calculated structure for the most stable conformer of $C_3F_7OONO_2$ and a table describing the energies and populations of the different conformers as well as two other tables dealing with the UV absorption cross sections. This information is available free of charge via the Internet at http://pubs.acs.org.

■ AUTHOR INFORMATION

Corresponding Author

*E-mail: fmalanca@fcq.unc.edu.ar.

Notes

The authors declare no competing financial interest.

■ ACKNOWLEDGMENTS

Financial support from SECYT-UNC, ANPCyT, and CONICET is gratefully acknowledged. A.B. thanks CONICET for a PhD fellowship.

■ REFERENCES

(1) Giessing, A. M. B.; Feilberg, A.; Møgelberg, T. E.; Sehested, J.; Bilde, M.; Wallington, T. J.; Nielsen, O. J. *J. Phys. Chem.* **1996**, *100*, 6572−6579.
(2) Wallington, T. J.; Schneider, W. F.; Worsnop, D. R.; Nielsen, O. J.; Sehested, J.; Debruyn, W. J.; Shorter, J. A. *Environ. Sci. Technol.* **1994**, *28*, 320−326.
(3) Chiappero, M. S.; Burgos Paci, M. A.; Argüello, G. A.; Wallington, T. J. *Inorg. Chem.* **2004**, *43*, 2714−2716.
(4) Malanca, F. E.; Chiappero, M. S.; Argüello, G. A.; Wallington, T. J. *Atmos. Environ.* **2005**, *39*, 5051−5057.
(5) Lee, C.; Yang, W.; Parr, R. G. *Phys. Rev. B* **1988**, *37*, 785−789.
(6) Hnyk, D.; Machácek, J.; Argüello, G. A.; Willner, H.; Oberhammer, H. *J. Phys. Chem. A* **2003**, *107*, 847−851.
(7) Mayer, F.; Oberhammer, H.; Berkei, M.; Pernice, H.; Willner, H.; Bierbrauer, K.; Burgos Paci, M.; Argüello, G. A. *Inorg. Chem.* **2004**, *43*, 8162−8168.
(8) Della Vedova, C. O.; Boese, R.; Willner, H.; Oberhammer, H. *J. Phys. Chem. A* **2004**, *108*, 861−865.
(9) Frisch, M. J.; Trucks, G. W.; Schlegel, H. B.; Scuseria, G. E.; Robb, M. A.; Cheeseman, J. R.; Zakrzewski, V. G.; Montgomery, J. A.; Stratmann, R. E.; Burant, J. C.; Dapprich, S.; Millam, J. M.; Daniels, A. D.; Kudin, K. N.; Strain, M. C.; Farkas, O.; Tomasi, J.; Barone, V.; Cossi, M.; Cammi, R.; Mennucci, B.; Pomelli, C.; Adamo, C.; Clifford, S.; Ochterski, J.; Petersson, G. A.; Ayala, P. Y.; Cui, Q.; Morokuma, K.; Malick, D. K.; Rabuck, A. D.; Raghavachari, K.; Foresman, J. B.; Cioslowsk, J.; Ortiz, J. V.; Stefanov, B. B.; Liu, G.; Liashenko, A.; Piskorz, P.; Komaromi, I.; Gomperts, R.; Martin, R. L.; Fox, D. J.; Keith, T.; Laham, Al M. A.; Peng, C. Y.; Nanayakkara, A.; Gonzalez, C.; Challacombe, M.; Gill, P. M. W.; Johnson, B. G.; Chen, W.; Wong, M. W.; Andres, J. L.; Gordon, Head M.; Replogle, E. S.; Pople, J. A. *Gaussian 98*, revision A.7; Gaussian, Inc.: Pittsburgh, PA, 1998.
(10) Dennington, R., Keith, T. Millam, J. *GaussView*, version 5; Semichem Inc.: Shawnee Mission, KS, 2009.
(11) Gilbert, R. G.; Smith, S. C.; Jordan, M. J. T. *UNIMOL program suite*; School of Chemistry, Sydney University, New South Wales, Australia, 2006.
(12) Ianni, J. C. *KINTECUS*, Windows version 2004, 3.7.
(13) Bossolasco, A. G.; Malanca, F. E; Argüello, G. A. *J. Photochem. Photobiol. A: Chem.* **2012**, *231*, 45−50.
(14) Chamberlain, G. A.; Whittle, E. *J. Chem. Soc., Faraday Trans 1* **1972**, *68*, 88−95.
(15) Chamberlain, G. A.; Whittle, E. *J. Chem. Soc., Faraday Trans 1* **1972**, *68*, 96−103.
(16) Kopitzky, R.; Beuleke, M.; Balzer, G.; Willner, H. *Inorg. Chem.* **1997**, *36*, 1994−1997.
(17) Scheffler, D.; Schaper, I.; Willner, H.; Mack, H. G.; Oberhammer, H. *Inorg. Chem.* **1997**, *36*, 339−344.
(18) Kopitzky, R.; Willner, H.; Mack, H. G.; Pfeiffer, A.; Oberhammer, H. *Inorg. Chem.* **1998**, *37*, 6208−6213.
(19) Casper, B.; Dixon, D. A.; Mack, H.-G.; Ulic, S. E.; Willner, H.; Oberhammer, H. *J. Am. Chem. Soc.* **1994**, *116*, 8317−8321.

(20) Okabe, H. *Photochemistry of small molecules*; Wiley: New York, 1978.
(21) Christensen, L. K.; Wallington, T. J.; Guschin, A.; Hurley, M. D. *J. Phys. Chem. A* **1999**, *103*, 4202−4208.
(22) Gilbert, G. R.; Smith, S. C. *Theory of Unimolecular and Recombination Reactions*; Blackwell Scientific Publications, Oxford, UK, 1990.
(23) Scott, A. P.; Radom, L. *J. Phys. Chem.* **1996**, *100*, 16502−16513.
(24) Mayer-Figge, A.; Zabel, F.; Becker, K. H. *J. Phys. Chem.* **1996**, *100*, 6587−6593.
(25) Pagsberg, P.; Jodkowski, J. T.; Ratajczak, E.; Sillesen, A. *Chem. Phys. Lett.* **1998**, *286*, 138−144.
(26) Roberts, J. M. PAN and Related Compounds. In *Volatile Organic Compounds in the Atmosphere*; Koppmann, R., Ed.; Blackwell Publishing Ltd, Oxford, UK., 2007.
(27) Talukdar, R. K.; Burkholder, J. B.; Schmoltner, A. M.; Roberts, J. M.; Wilson, R. R.; Ravishankara, A. R. *J. Geophys. Res.* **1995**, *100*, 14163−14173.